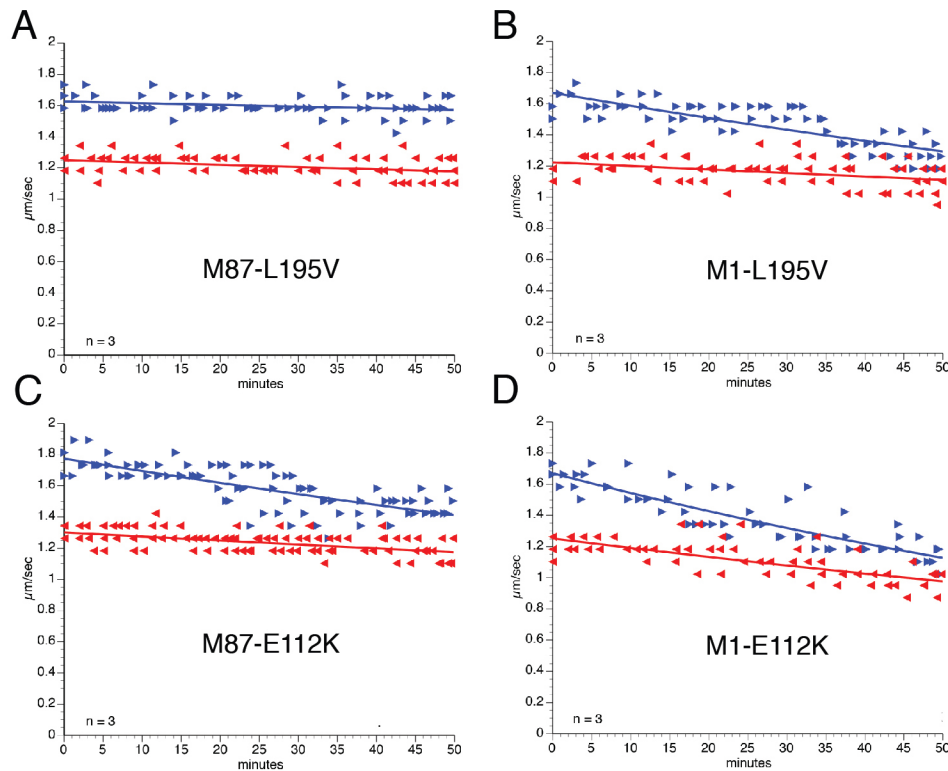


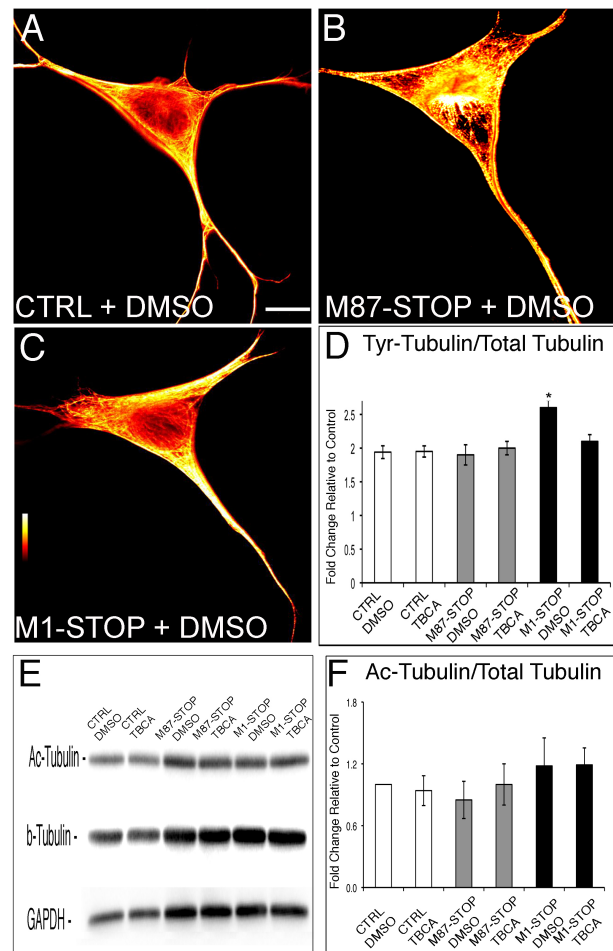
*“Mutant spastin proteins promote deficits in axonal transport through an isoform-specific mechanism involving casein kinase 2 activation”* Lanfranco Leo, Carina Weissmann, Matthew Burns, Minsu Kang, Yuyu Song, Liang Qiang, Scott T. Brady, Peter W. Baas, and Gerardo Morfini.

### Supplementary Material



#### Suppl. Material Figure S1: Effects of M1 and M87 spastins bearing L195 and E112K mutations on FAT.

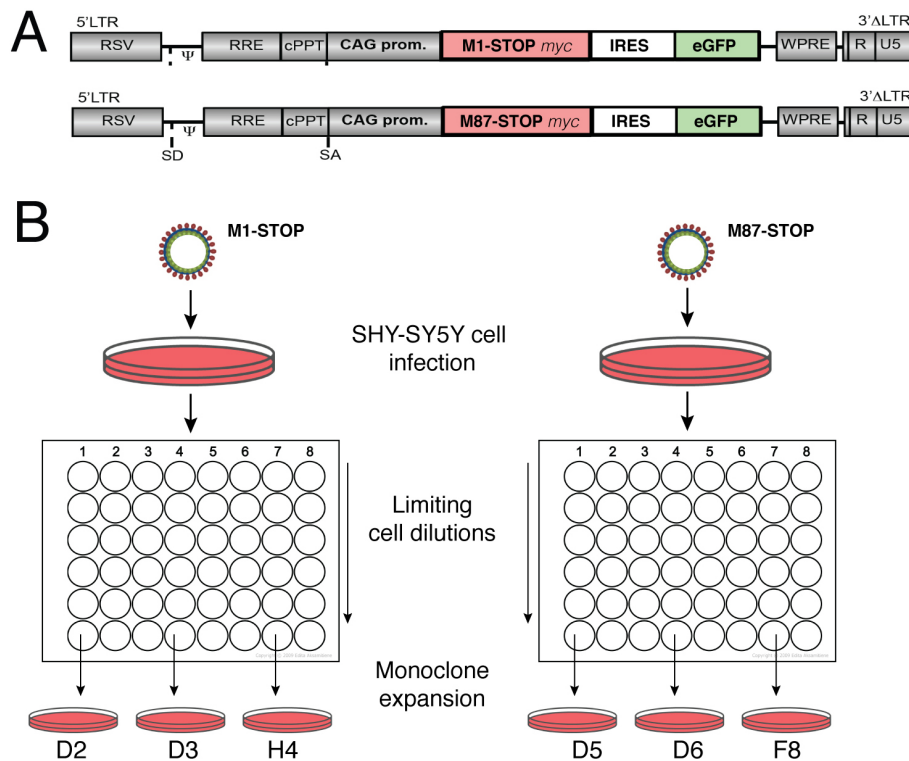
Plots in A-D depict results from vesicle motility assays in isolated squid axoplasm. *In vitro* translated mutant spastins were perfused and fast axonal transport (FAT) rates monitored by video microscopy. Individual rate measurements ( $\mu\text{m}/\text{s}$ , arrowheads) are plotted as a function of time (minutes). Both anterograde (blue arrowheads and lines) and retrograde (reverse red arrowheads and lines) FAT rates are shown in each plot. Perfusion of the SPG4-HSP-related mutant spastin proteins M87-L195V (A) and M1-E112K (C) in isolated squid axoplasm did not affect FAT rates. In contrast, perfusion of their M1-L195V (B) and M1-L195V (C) isoform counterparts inhibited both anterograde and retrograde FAT rates. Quantitation of average FAT rates in A-D is shown in **Figs 1 G-H**. n: number of independent experiments.



**Suppl. Material Figure S2: Analysis of tubulin post-translational modifications in M1-STOP and M87-STOP neuroblastoma cells.** (A-C) An increase (of approximately 30%) in tubulin tyrosination is indicated by immunocytochemistry in cells expressing M1-STOP (C;  $2.6 \pm 0.11$  tyrosinated tubulin to total tubulin ratio) compared to cells expressing M87-STOP (B) or control cells (A) ( $1.94 \pm 0.11$  and  $1.92 \pm 0.15$  ratio values, respectively). As shown in D, tyrosinated tubulin levels in the presence of TBCA was the same in all groups (M1-STOP + TBCA:  $2.1 \pm 0.10$ ; M87-STOP + TBCA:  $2.0 \pm 0.10$ ; control + TBCA:  $1.95 \pm 0.08$ ) and statistically indistinguishable from DMSO-treated control and M87-STOP groups, indicating that the increase in tyrosinated tubulin due to M1-STOP was correctable by TCBA treatment. Ratio images in A-C are shown in fire scale, with white being the most intense and red being the least intense. (E-F) Quantitative Western blot shows no significant changes in acetylated tubulin/total tubulin ratios: M87-STOP+DMSO ( $1.18 \pm 0.47$ ) and M1-STOP+DMSO ( $0.9 \pm 0.31$ ). No significant changes in tubulin acetylation were observed after treatment with TBCA (control+TBCA:  $0.9 \pm 0.25$ ; M1-STOP+TBCA:  $1.0 \pm 0.35$ ; M87-STOP+TBCA:  $1.2 \pm 0.29$ ).

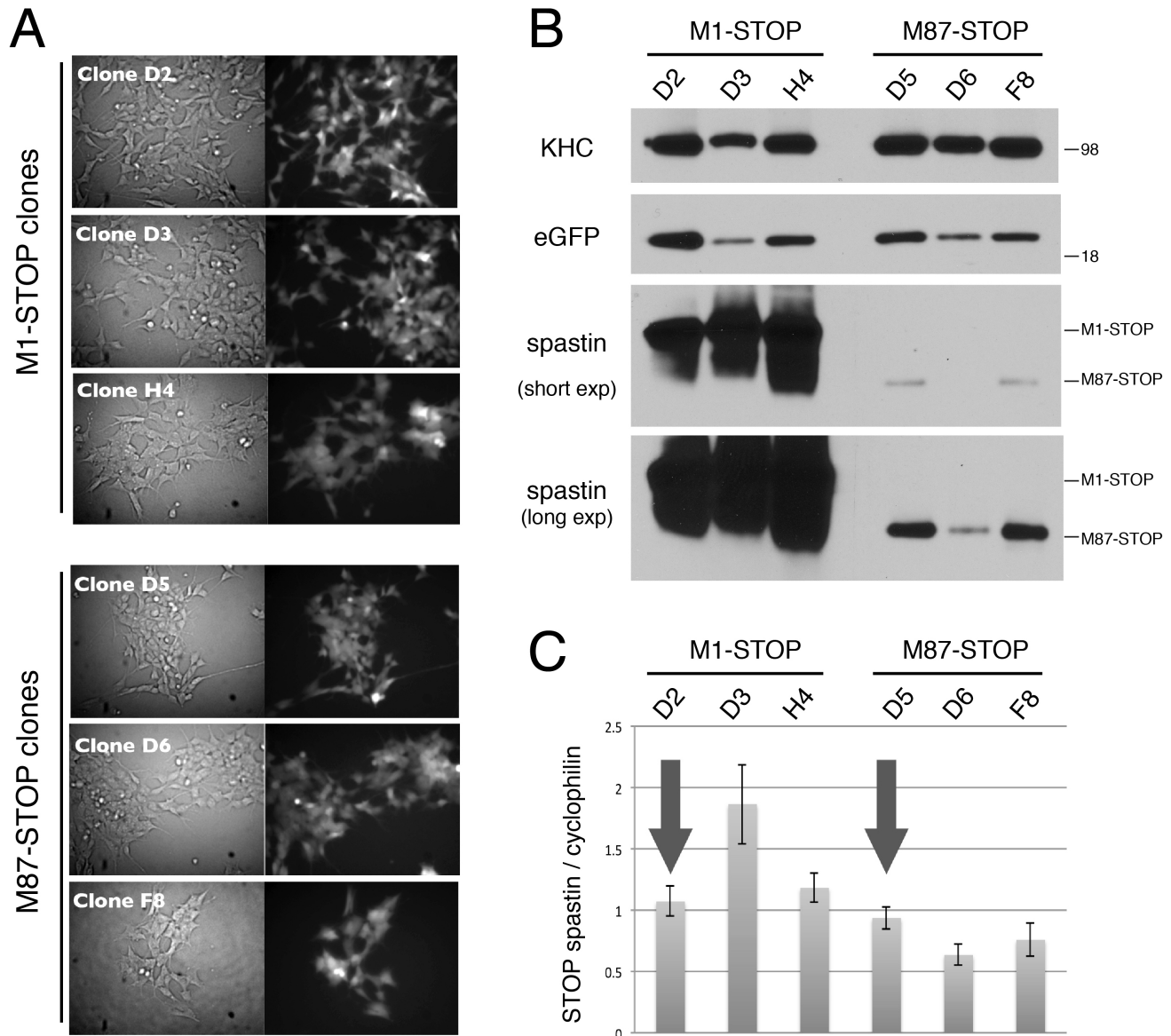
## Supplementary Methods

**Generation of lentiviral constructs:** cDNA constructs encoding myc-tagged M1-STOP or M87-STOP mutant spastin proteins were sub-cloned in the bicistronic lentiviral plasmid vector FCbAGW-IRES-eGF. Generated by introducing an IRES sequence in the original FCbAGW-eGFP vector (1), FCbAGW-IRES-eGFP allows for simultaneous expression of STOP spastin transgenes (M1-STOP or M87-STOP) and eGFP (**Suppl. Meth. Fig. 1A**). Lentiviral particles were prepared by calcium phosphate-based co-transfection of HEK293 cells with FCbAGW-IRES-GFP, VSVg and DeltaR8.9 helper plasmids, and used to infect undifferentiated SH-SY5Y cells. 48 hours after infection, cells were detached from culture dishes and limited dilutions of eGFP-positive cells performed using 96-well plates. For each STOP spastin construct, three monoclones were selected for each STOP spastin cell line. These clones (D2, D3, and H4 clones for M1-STOP and D5, D6, and F8 for M87-STOP) were expanded for further characterization (**Suppl. Meth. Fig. 1B**).



**Suppl. Methods Figure S1:** **A)** Schematics describing FCbAGW-STOPspastin-IRES-eGFP lentiviral constructs. **B)** Outline of procedures for the generation of monoclonal cells expressing M1-STOP or M87-STOP.

**Immunoblot analysis of STOP spastin proteins.** After repeated passages, brightfield and fluorescence imaging analysis of SH-SY5Y monoclonal lines revealed robust eGFP expression and no obvious changes in morphology and viability (**Suppl. Meth. Fig. 2A**). Expression levels of transgenic STOP spastins were evaluated by immunoblotting using a monoclonal antibody against spastin (6c6 clone, **Suppl. Meth. Fig. 2A**). Levels of transgenic M1-STOP protein expression were significantly higher than those of M87-STOP. Small variations in eGFP expression levels were found among the clones analyzed, but those did not correlate with changes in STOP spastin expression. Because eGFP expression in each clone is driven by an IRES promoter located immediately downstream of STOP spastins (**Suppl. Methods Fig. 1A**), these results suggested differences in processing and/or stability of M1-STOP and M87-STOP proteins. Based on these observations, we performed semi-quantitative PCR experiments to evaluate whether differences in M1-STOP and M87-STOP protein expression resulted from differential stability of transgene mRNAs (2). To this end, differentiated M87-STOP and M1-STOP cells were lysed using Trizol reagent (Thermo Fisher), and mRNAs purified using phenol/chloroform separation followed by isopropanol precipitation. After treatment with DNase (Promega), cDNAs were generated using iScript Synthesis kit (Bio-Rad), following the manufacturer procedures. Using PrimerQuest primer design software (Integrated DNA Technologies), primers were designed to amplify transgenic STOP spastin mRNAs (forward: 5'-AATTTGGTTATGGCCAAGGACCGC-3'; reverse: 5'-CCATTGCGGCATGCCAAGTTAGTA-3') and the housekeeping gene cyclophilin (forward: 5'-GCAGACAAGGTCCCAAAGACAG-3'; reverse: 5'-CACCTGACACATAAACCTGG-3'). Plots shown in **Suppl. Meth. Fig. 2C** depict STOP spastin/cyclophilin mRNA ratios. While some small variation in the relative expression levels of STOP spastin mRNAs was observed among different clones, such differences did not parallel those observed for STOP spastin protein expression. Further, levels of translated M1-STOP spastin protein were much higher for M1-STOP clones D2 and H4 than M87-STOP clone D5, despite comparable levels of STOP spastin mRNA expression. Collectively, these results indicate differences in the processing and/or stability of STOP spastin isoforms rather than differences in mRNA levels, consistent with our prior report documenting increased levels of mutant M1 spastin protein in *SPG4*-HSP spinal cord tissue (3).

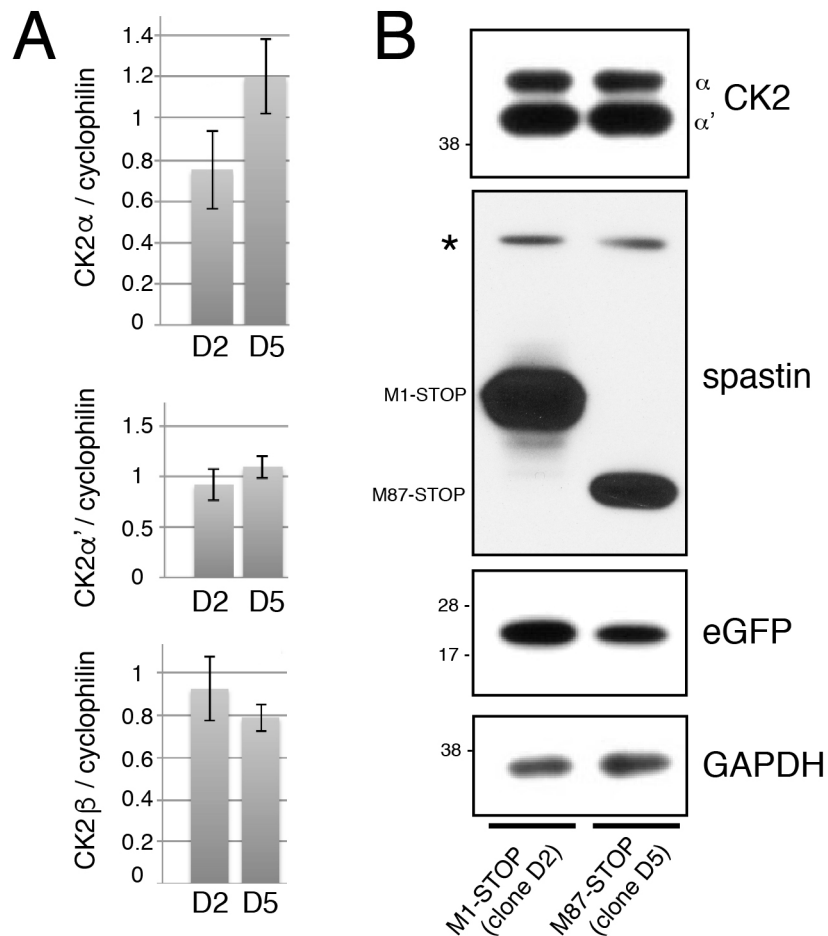


**Suppl. Methods Figure S2:** (A) Brightfield (left panels) and corresponding fluorescent (right panels) images reveal robust eGFP expression and similar morphology for all M1-STOP and M87-STOP clones analyzed. (B) SH-SY5Y cell monoclonal expressing M1-STOP and M87-STOP were analyzed by immunoblotting using antibodies against spastin [6c6 clone(4)], GFP (Molecular Probes, cat#A11121), and kinesin heavy chain [KHC, H2 monoclonal antibody (5, 6)]. Short and long film exposures are shown for anti-spastin 6c6 antibody. (C) Plots depict results from quantitative PCR analysis. of transgenic STOP spastin mRNA expression levels. Cyclophilin mRNA levels were used for normalization. Note that same levels of M1-STOP and M87-STOP mRNA expression were found for clones D2 and D5, respectively (arrows).

**Characterization of M1-STOP (D2) and M87-STOP (D5) SH-SY5Y cells.** Based on analysis of spastin mRNA and protein expression, we selected M1-STOP clone D2 and M87-STOP clone D5, which express comparable

levels of STOP spastin mRNAs, for further characterization (**Suppl. Meth. Fig. 2C**).

qPCR analysis was performed using primers that selectively amplify mRNAs encoding casein kinase 2 (CK2) subunits CK2 $\alpha$ , CK2 $\alpha'$ , and CK2 $\beta$ . Plots shown in **Suppl. Meth. Fig. 3A** depict relative levels of these mRNAs normalized to cyclophilin mRNA levels. A slight increase in CK2 $\alpha$  mRNA levels was observed for D5 cells, compared to D2 cells, whereas CK2  $\alpha'$ , and  $\beta$  mRNA levels were similar. Immunoblotting analysis using a polyclonal that selectively recognize CK2 $\alpha$  and  $\alpha'$  subunits confirmed similar levels of expression for these proteins among M1-STOP (D2) and M8-STOP7 (D5) cell lines (**Suppl. Meth. Fig. 3B**).



**Suppl. Methods Figure S3:** (A) Plots depict results from quantitative PCR analysis of CK2 $\alpha$ ,  $\alpha'$ , and  $\beta$  subunit mRNA expression in M1-STOP (clone D2) and M87-STOP (clone D5) cells. Cyclophilin mRNA levels were used for normalization. (B) Immunoblot analysis showed similar levels of CK2 $\alpha$ , and  $\alpha'$  protein expression among these cell lines. An asterisk indicates endogenous SH-SY5Y spastin.

**Supplementary Table 1**

<b>Anterograde FAT rates</b>						
<b>Experiment</b>	<b><i>n</i></b>	<b># rate measurements</b>	<b>Av. Rate (µm/sec)</b>	<b>Variance</b>	<b>Std Dev</b>	<b>Std Err</b>
M1- STOP	3	19	1.28947	0.018639	0.136523	0.031321
M1- STOP + TBCA	3	31	1.46645	0.011424	0.106882	0.019196
M1- STOP + CK2pept	3	30	1.63767	0.003743	0.061177	0.011169
M87-STOP	2	21	1.61810	0.001676	0.040941	0.008934
M1-E442Q	2	23	1.19913	0.010163	0.100811	0.021021
M1-E442Q + TBCA	3	35	1.53657	0.006153	0.078439	0.013259
M87-E442Q	2	24	1.53000	0.009357	0.096729	0.019745
M1-C448Y	3	26	1.25692	0.006390	0.079938	0.015677
M1-C448Y + TBCA	4	29	1.43379	0.015574	0.124797	0.023174
M87-C448Y	3	28	1.46286	0.029621	0.172108	0.032525
M1-L195V	3	29	1.35655	0.015716	0.125364	0.023280
M87-L195V	3	29	1.58517	0.004890	0.069930	0.012986
M1-E112K	3	26	1.22308	0.015478	0.124411	0.024399
M87-E112K	3	32	1.46750	0.006961	0.083434	0.014749

<b>Retrograde FAT rates</b>						
<b>Experiment</b>	<b><i>n</i></b>	<b># rate measurements</b>	<b>Av. Rate (µm/sec)</b>	<b>Variance</b>	<b>Std Dev</b>	<b>Std Err</b>
M1- STOP	3	20	1.01880	0.005950	0.077139	0.017249
M1- STOP + TBCA	3	30	1.22000	0.005186	0.072015	0.013148
M1- STOP + CK2pept	3	31	1.23677	0.002216	0.047073	0.008455
M87-STOP	2	21	1.25238	0.003779	0.061474	0.013415
M1-E442Q	2	24	1.01904	0.005404	0.073509	0.015005
M1-E442Q + TBCA	3	35	1.21429	0.009896	0.099478	0.016815
M87-E442Q	2	25	1.24400	0.003200	0.056569	0.011314
M1-C448Y	3	26	1.09138	0.008171	0.090394	0.017728
M1-C448Y + TBCA	4	28	1.13011	0.018789	0.137074	0.025905
M87-C448Y	3	29	1.17448	0.012311	0.110956	0.020604
M1-L195V	3	29	1.13090	0.010947	0.104629	0.019429
M87-L195V	3	30	1.19067	0.005620	0.074968	0.013687
M1-E112K	3	26	1.02285	0.008643	0.092969	0.018233
M87-E112K	3	32	1.20250	0.005052	0.071075	0.012564

***n***: Number of independent experiments.

**# rate measurements**: Number of independent FAT rate measurements obtained from 30-50 minutes after perfusion.

**Av. Rate**: Average FAT rate.

**St Dev**: Standard deviation.

**Std Err**: Standard error.

## REFERENCES

- 1 Dittgen, T., Nimmerjahn, A., Komai, S., Licznanski, P., Waters, J., Margrie, T.W., Helmchen, F., Denk, W., Brecht, M. and Osten, P. (2004) Lentivirus-based genetic manipulations of cortical neurons and their optical and electrophysiological monitoring in vivo. *Proc Natl Acad Sci U S A*, **101**, 18206-18211.
- 2 Charvin, D., Cifuentes-Diaz, C., Fonknechten, N., Joshi, V., Hazan, J., Melki, J. and Betuing, S. (2003) Mutations of SPG4 are responsible for a loss of function of spastin, an abundant neuronal protein localized in the nucleus. *Hum Mol Genet*, **12**, 71-78.
- 3 Solowska, J.M., Garbern, J.Y. and Baas, P.W. (2010) Evaluation of loss of function as an explanation for SPG4-based hereditary spastic paraplegia. *Hum Mol Genet*, **19**, 2767-2779.
- 4 Salinas, S., Carazo-Salas, R.E., Proukakis, C., Cooper, J.M., Weston, A.E., Schiavo, G. and Warner, T.T. (2005) Human spastin has multiple microtubule-related functions. *J Neurochem*, **95**, 1411-1420.
- 5 Brady, S.T., Pfister, K.K. and Bloom, G.S. (1990) A monoclonal antibody against kinesin inhibits both anterograde and retrograde fast axonal transport in squid axoplasm. *Proc. Nat. Acad. Sci. USA*, **87**, 1061-1065.
- 6 DeBoer, S.R., You, Y., Szodorai, A., Kaminska, A., Pigino, G., Nwabuisi, E., Wang, B., Estrada-Hernandez, T., Kins, S., Brady, S.T. *et al.* (2008) Conventional kinesin holoenzymes are composed of heavy and light chain homodimers. *Biochemistry*, **47**, 4535-4543.